J Appl Phycol (2017) 29:1865–1875
DOI 10.1007/s10811-017-1091-9

Biogenic synthesis and characterization of silver nanoparticles and their effects against bloom-forming algae and synergistic effect with antibiotics against fish pathogenic bacteria

Smrutirekha Satapathy[1] · **Saurav Kumar**[1] · **Kapil S. Sukhdane**[2] · **Satya Prakash Shukla**[1]

Received: 8 August 2016 / Revised and accepted: 8 February 2017 / Published online: 5 April 2017

Abstract The present work evaluates the bacteriocidal and algicidal efficacy of nanosilver particles (AgNPs) synthesized through a green pathway by using the cyanobacterium *Synechococcus elongatus*. Further, the synergistic effects of the conjugates of selected antibiotics and biogenic silver nanoparticle were evaluated against three Gram-negative fish pathogens, viz. *Aeromonas hydrophila* ATCC-7966, *Vibrio parahaemolyticus* ATCC BAA-238 and *Edwardsiella tarda* ATCC-15947. The biogenic silver nanoparticles were polydispersed and showed a size range 71–201 nm with a zeta potential of −9.11 mV. The antibacterial activities of ampicillin, gentamicin, ofloxacin and ciprofloxacin exhibited a significant ($P < 0.05$) increase when conjugated with AgNPs against the selected bacterial strains. The highest synergistic effect of conjugates of AgNPs with gentamicin and ampicillin was observed against *E. tarda*. The biogenic silver nanoparticles exhibited a considerable inhibition of growth and decrease in photosynthetic pigments in a bloom-forming alga (*Microcystis aeruginosa*) and biofouling alga (*Phormidium* sp). This report aims to establish that biogenic silver nanoparticles are effective against water-borne fish pathogens and their efficacy is comparable with silver nanoparticles synthesized through chemical-based pathways. Since most of the reports on antibacterial properties of silver nanoparticles are on human pathogens, this report will provide baseline data for aquatic pathogens which result in a considerable loss of fish production due to disease outbreak.

Keywords Silver nanoparticle · *Synechococcus elongatus* · Green chemistry · Bactericidal and algicidal properties · Antibiotics

Introduction

Antimicrobials are widely used for disease cure in humans and growth promotion in animals including fish. In 2010, total consumption of antibiotics was 63,151 t (in 228 countries) and a 67% increase in consumption has been projected by 2030 (Van Boeckel et al. 2015). In Asia, antimicrobial consumption is projected to be 51,851 t and a considerable increase in the consumption has been projected for developing countries in 2030. In aquaculture, there is an intensive use of antibiotics either as an ingredient of medicated feed or in immersion therapy which involves direct application of antibiotics to the water (Heuer et al. 2009). Intensive use of antibiotics in aquaculture impacts a wide variety of bacteria in the environment if the effluents are not properly treated (Schwartz et al. 2003; Koonse et al. 2005). Inadequate effluent treatment practices for antibiotic removal lead to accumulation of residual antibiotics and its derivatives in the aquatic system which increases selective pressure on endemic bacterial strains in the aquatic environment. In view of the considerable increase in prevalence of antibiotic resistant bacteria, an increased consumption of antibiotics coupled with inadequate effluent treatment system may lead to further increase in number of such strains in the aquatic environment (WHO 2005). Considering the above, reduction in the quantity of antibiotics used in

Electronic supplementary material The online version of this article (doi:10.1007/s10811-017-1091-9) contains supplementary material, which is available to authorized users.

✉ Saurav Kumar
sauravsinha535@gmail.com

✉ Satya Prakash Shukla
spshukla@cife.edu.in

[1] ICAR-Central Institute of Fisheries Education, Versova, Mumbai 400061, India

[2] ICAR-Central Marine Fisheries Research Institute, Veraval, Gujarat, India

aquaculture and other sectors without compromising health security and production is a judicious approach to minimize the detrimental effects of antibiotics on the environment. Enhancement of antibiotic efficacy through synergism with metal nanoparticles has been explored recently to achieve the above goal (Sharma et al. 2009; Fayaz et al. 2010). Additionally, augmentation of the efficacy of antibiotics through conjugation with a specific metal nanoparticle is a scientific approach to check the increasing trend of antibiotic consumption worldwide. Metal nanoparticles (Me-NPs) have higher surface area to volume ratio to their natural form and, therefore, have received extensive attention in recent years because of their remarkable properties and wide range of applications in catalysis (Paul et al. 2014), plasmonics (Khlebtsov and Dykman 2010), optoelectronics (Muruganandam et al. 2014), biological sensors (Venkatesan and Santhanalakshmi 2014), water treatment (Con and Loan 2011) and pharmaceutical applications (Ravichandran 2009; Roychoudhury et al. 2016). Among Me-NPs, silver nanoparticles (AgNPs) have been identified for algicidal (Dash et al. 2012) and bactericidal effects against pathogenic microorganisms (Cho et al. 2005). In view of increasing demand for AgNPs, various physical and chemical methods have been developed for synthesis and preparation of nanosilver particles; however, most of these methods are not eco-friendly due to their toxic by-products (Singaravelu et al. 2007). In view of the toxic nature and hazardous waste generated during the synthetic chemical- and radiation-based pathways, nanoparticle synthesis using biological materials has gained considerable importance (Kannan et al. 2013). Biological entities ranging from bacteria to fungi and algae to higher plants have shown the potentialities for green synthesis of metal nanoparticles and revealed many advantages of green pathways (Rai et al. 2012; Sharma et al. 2016). A systematic approach to study the synthesis of metal nanoparticles by algae was initiated using a phaeophycean alga *Sargassum wightii* (Singaravelu et al. 2007). The cyanobacterium *Spirulina (Arthrospira) platensis* was also found capable of synthesizing silver, gold and bimetallic nanoparticles when reacted with $AgNO_3$ and $HAuCl_4$ (Govindaraju et al. 2008). Among the marine macroalgae, *Cystophora moniliformis* and *Laurencia* spp. showed a potential for their use as a reducing and stabilizing agent for the synthesis of biogenic silver nanoparticle (Prasad et al. 2013, Vieira et al. 2016). The metallic and biogenic silver nanoparticles produced by reduction of aqueous Ag^+ and *Ulva fasciata*, respectively, showed a remarkable synergistic effect with selected antibiotics against human Gram-positive and Gram-negative bacteria (Shahverdi et al. 2007; Fayaz et al. 2010). Although there are an appreciable number of reports on synergistic effects of metal nanoparticles on human pathogens, baseline information about the efficacy of antibiotics conjugated with metal nanoparticles against aquatic bacterial strains, especially fish pathogenic strains, is not available in the literature. Therefore, the present investigation will facilitate in filling the gaps in knowledge pertaining to synergistic effects of antibiotics and metal nanoparticles against bacterial fish pathogens. Moreover, the algicidal property of biogenic silver nanoparticles is still a little explored area of research. Park et al. (2010) attempted to evaluate the efficacy of silver nanoparticle against a toxic bloom-forming cyanobacterium *Microcystis aeruginosa*. However, the silver nanoparticle produced for the above study was synthesized using tannic acid and sodium persulphate. Therefore, this report provides preliminary new information about the selective inhibition of growth of *M. aeruginosa* through biogenic silver nanoparticles synthesized through a green approach. Recently, Zhang et al. (2014) found silver nanoparticle synthesized by *Lactobacillus fermentum* effective in inhibiting the colonization of a biofouling bacterium *Pseudomonas aeruginosa*. A similar phenomenon has been reported by Martinez-Gutierrez et al. (2013). Since algae are major components of biofouling assemblages, this report also provides data on the inhibition of growth of a marine fouling cyanobacterium *Phormidium fragile* by graded concentrations of biogenic silver nanoparticles.

Materials and methods

Unialgal populations of *Synechococcus elongatus* Nägeli were isolated from water samples from a crater lake (Lonar Lake, Maharashtra, India; 19.975° N; 76.506° E) following the standard protocol for isolation and culture maintenance (Guillard 1973). The biomass of the organism was produced in an air-lift culture assembly consisting of a 20-L aspirator bottle fitted with an air-injection device. The air passing through the culture was decontaminated by a sintered glass air filter. The culture in the reservoir was continuously stirred (100 rpm) with the help of a magnetic stirrer. Algal material was washed thoroughly with tap water and distilled water to remove extraneous materials and was shade-dried for 5 days followed by oven-drying at 60 °C until constant weight was obtained. The dried biomass was then minced into fine powder using an electric mixer and stored at 4 °C for experimental use.

The marine algal species of *Phormidium fragile* Gomont was isolated from a heterogeneous assemblage of algae collected from the surface of boats of Versova Fish Landing Centre, Mumbai, India. Streak plating technique was followed to isolate the unialgal cultures. Pure cultures of freshwater species were maintained in BG 11 medium (Stanier et al. 1971), and the marine species *P. fragile* was sub-cultured in ASW (artificial sea water) medium (Guillard and Ryther 1962). The unialgal populations were maintained at temperature 24 ± 2 °C with an illumination of 54 μmol photons m^{-2} s^{-1}. The photoperiod was 12: 12 h light and dark.

Biosynthesis of nanosilver particles

Fifteen litre of exponential phase culture of *S. elongatus* with an initial density of 350 μg mL^{-1} protein was exposed to 10^{-3} M $AgNO_3$ (silver nitrate) following the procedure described earlier (Satapathy et al. 2015). The conversion of silver ions into metallic silver was monitored by ultraviolet–visible (UV–vis) absorption measurement in 200–750-nm range using a spectrophotometer (Thermospectronic, UK; UV-1 model). The formation of silver nanoparticles was confirmed by measuring the absorption maxima of the supernatant of the algal suspension spiked with silver nitrate (10^{-3} M) which showed a peak absorbance at 400 nm due to shift in surface plasmon resonance, imparting a brown colour to the solution. For the characterization of silver nanoparticles, the brown colour solution was concentrated at 60 °C to reduce the volume. The concentrated solution was centrifuged at 15,900×*g* for 30 min. The pellet obtained was washed with deionized water and centrifuged again for 15 min. The process was repeated to remove water-soluble biomolecules from AgNP suspension.

Characterization of biogenic silver nanoparticles

The size of the silver nanoparticles was measured by a particle size analyser (Malvern Mastersizer 2000) and transmission electron microscopy. For TEM, a drop of the solution after sonication for 5 min in a sonicator bath was placed on a carbon-coated copper grid and dried. The grid was scanned using a Phillips Tecnai-20 model transmission electron microscope operated at 100 kV. Solution-cast films were used for Fourier transform infrared spectroscopy (FTIR). Samples were prepared by drop-coating method on a smooth NaCl crystal. The spectra of samples were recorded by Perkin Elmer spectrometer (Model 100 FTIR) in the range 4000 to 400 cm^{-1}. Zeta potential was measured using a Beckman Coulter DELSA Nano C Particle Analyser. For X-ray diffraction analysis, a colloidal solution of silver nanoparticles was prepared by repeated centrifugation at 15,900×*g* for 15 min and redispersion in deionized water (Millipore, USA). The samples were analysed using XPERT-PRO diffractometer (PANalytical, Netherlands) operated at 45 kV, 40 mA generator settings. The start and end positions for 2° theta were 2.0134 and 49.9874, respectively.

In vitro antibacterial assay and disc diffusion assay to evaluate synergistic effects

The pathogenic fish bacterial strains *Aeromonas hydrophila* ATCC 7966, *Edwardsiella tarda* ATCC 15947 and *Vibrio parahaemolyticus* ATCC BAA-238 were obtained from Aquatic Animal Health Management Division, ICAR-CIFE, Mumbai, India. The bacterial strains tested during the study were inoculated in 5 mL of Mueller-Hinton broth (MHB) from the stock culture and incubated overnight at 28 °C. The culture broth was centrifuged at 8000×*g* for 5 min at 4 °C, and the pellets were washed twice with PBS (phosphate-buffered saline, pH 7.4) and resuspended in 0.85% saline water. Turbidity was adjusted to 0.5 McFarland standards (10^8 CFU mL^{-1}) and was further confirmed by optical density (OD) determination. The antimicrobial activity of biogenic AgNPs was evaluated using standard protocols of disc diffusion methods (Bauer et al. 1966). The selected bacterial cultures were uniformly spread on Mueller-Hinton agar (HiMedia, India) with the help of a sterile glass spreader. Various antibiotic discs (HiMedia), disc containing 10^{-3} M AgNPs and in different combinations with antibiotics and biogenic AgNPs (gentamicin and ampicillin 100 μg per disc; ofloxacin and ciprofloxacin 5 μg per disc + 10^{-3} M), were placed on the plates and incubated at 28 °C for 24 h. The test was performed in triplicate. The growth of the bacteria was inhibited around the disc, and a clear zone around the circumference of the disc was observed. The diameter more than 8 mm of the growth-free zone was measured and considered as positive with HiMedia zone scale, and it corresponded to the size of the inhibition zone. The synergistic effect of AgNPs on antibiotics was measured as difference in size of inhibition zone (ZOI) of combination to antibiotics alone.

$$\text{Synergistic level (in\%)} = \frac{\text{ZOI [(AgNP + antibiotics)}-\text{(antibiotics)] in mm}}{\text{ZOI (antibiotics) in mm}} \times 100$$

Effect of biogenic silver nanoparticles on bloom-forming alga *Microcystis aeruginosa* (Kützing)

Algal samples were collected from Powai Lake, Mumbai, India. Microscopic examination showed that *M. aeruginosa* was the dominant species (almost 90% of the algal colonies/cells observed under Sedgwick-Rafter counter). About 40 L of lake water was passed through a plankton net (mesh size 70 μm) to concentrate the colonies of the organism. One hundred millilitres of this concentrated sample was transferred to a conical flask and then different concentrations 1–5% silver nanoparticle solution were added and the flasks were incubated in a plant growth chamber under illumination of 54 μmol photons m^{-2} s^{-1}. The samples were observed using a microscope, and colonies were counted using a Sedgwick-Rafter counting chamber.

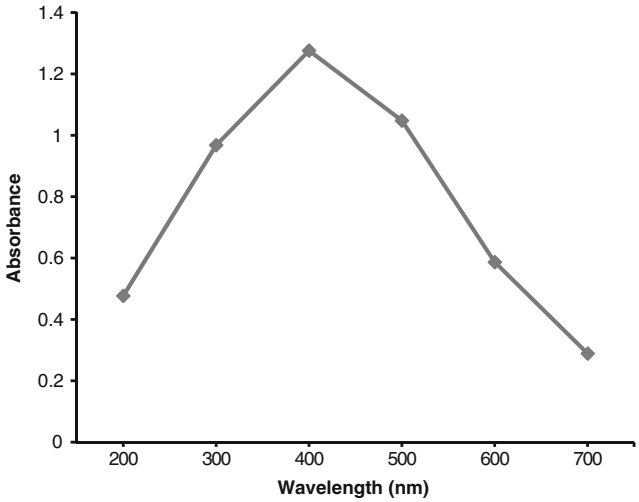

Fig. 1 UV–vis absorption spectrum of cell-free suspension of *S. elongatus* containing silver nanoparticles formed after bioreduction of silver nitrate (10^{-3} M). The peak at 400 nm depicts the transformation of ionic silver to AgNPs due to shift in plasmon resonance

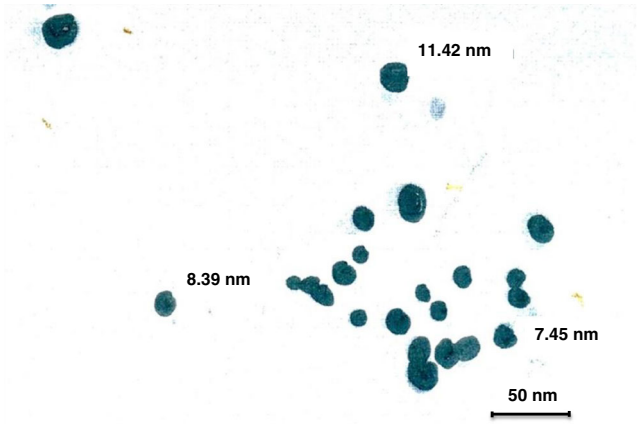

Fig. 3 Transmission electron microscopy image of silver nanoparticles synthesized after bioreduction through *S. elongatus* biomass

Growth measurement and chlorophyll estimation

The specific growth rate (k) of the algae was calculated by using the formula of Kratz and Myers (1955):

$$k_{(d^{-1})} = 2.303\ \frac{\log N_2 - \log N_1}{t_2 - t_1}$$

where k is the specific growth rate, N_1 is the initial number of cells at time t_1 and N_2 is the final number of cells at time t_2.

The generation time (G) (per day) was calculated using the formula:

$$G = \frac{0.693}{k}$$

Chlorophyll estimation Fifteen millilitre of algal culture was taken after 7 days of exposure with different concentrations of Ag nanoparticles used for toxicity experiment. The culture was centrifuged at 10,000×g for 15 min at 4 °C. The supernatant was discarded, and 15 mL of dimethyl formamide (DMF) was added to the remaining pellet and kept in a shaker for 3 h to break the cells. After complete extraction, it was again centrifuged at 5000 rpm for 15 min. The supernatant was collected and optical density was measured at 664 nm. Chlorophyll concentration was calculated using the formula (Moran 1982):

$$\text{Chlorophyll } a \text{ concentration in } \mu\text{g mL}^{-1} = \text{OD}_{664} \times 11.92$$

Statistical analysis

The data of antibacterial activity of various combinations of AgNPs and antibiotics were statistically analysed using

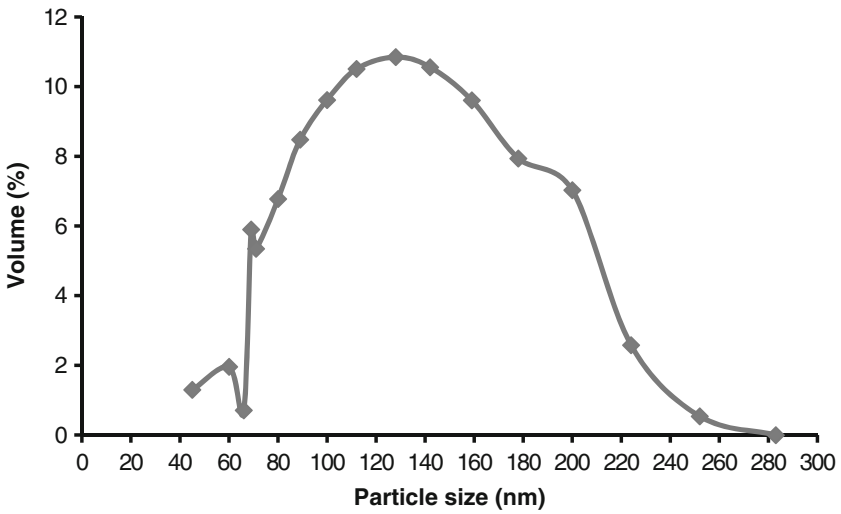

Fig. 2 Size distribution of silver nanoparticles biosynthesized through *S. elongatus* measured with a particle size analyser

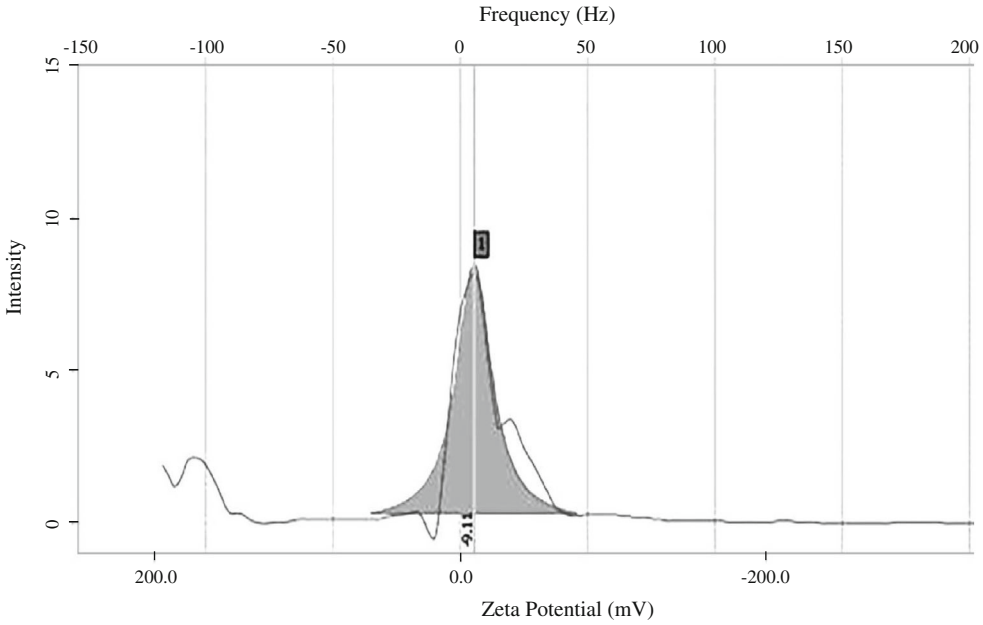

Fig. 4 Zeta potential of silver nanoparticles synthesized through *S. elongatus*

statistical package SPSS version 16 by one-way ANOVA and Duncan's multiple range tests to determine the significant differences between the means. Comparisons were made at 5% probability level.

Results

Biosynthesis of nanosilver particles

The UV–visible spectrograph (Fig. 1) of the algal suspension treated with 10^{-3} M silver nitrate showed a shift in absorption peak to 400 nm after 72 h. The colour of the suspension also changed to brown, indicating a shift in surface plasmon resonance (SPR) of silver ions after bioreduction.

Characterization of biogenic AgNPs

The size distribution of the biogenic silver nanoparticle shows that the size of nanoparticle was up to 201 nm. Among these, 10% nanoparticles were up to 71 nm and 50% were up to 125 nm in size (Fig. 2). However, the TEM micrographs of the silver nanoparticle show that the majority of AgNPs were in the size range 7–12 nm, with an average size 10.48 nm (n = 20) (Fig. 3). The zeta potential of silver nanoparticles produced from *S. elongatus* was −9.11 mV (Fig. 4) with

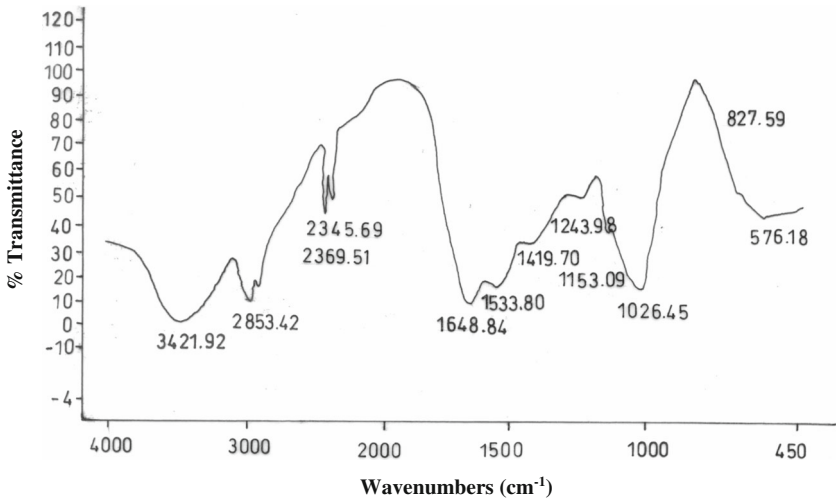

Fig. 5 Fourier transform infrared spectrum (4000 to 450 cm^{-1}) of the untreated biomass showing different bands corresponding to the presence of various functional groups

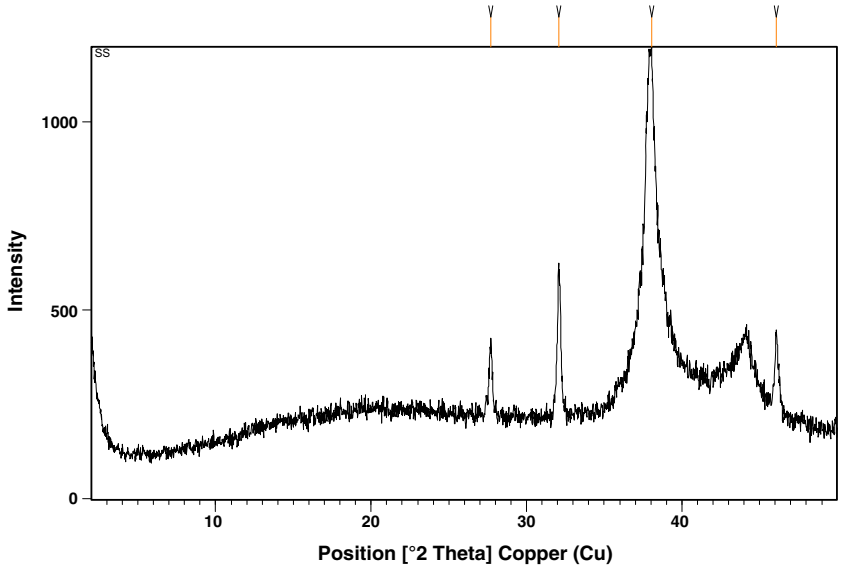

Fig. 6 X-ray diffraction spectrum of the treated biomass of *S. elongatus* showing the sharp peak at 38.06° Bragg's angle depicting the dominance of (111) planes of silver nanoparticles

conductivity 2.3008 mS cm^{-1}. The presence of some functional groups as revealed by (FTIR) spectral analysis is shown in Fig. 5. FTIR analyses of the dried algal biomass of *S. elongatus* after silver nitrate treatment showed shifting of bands corresponding to various functional groups in the bioreduction process. FTIR measurements show 11 intense bands at 3421.92 (O–H stretch of alcohols), 2853.42 (C–H stretch of alkane), 2345.69 and 2369.51 (O–H stretch of carboxylic acid), 1648.84 and 1533.80 (N–H band of amide), 1419.70 (O–H band of carboxylic acid), 1243.90 (C-O stretch of carboxylic acid), 1026.45 (C–O stretch of alcohols), 827.57 (C–H band of aromatics) and 576.18 cm^{-1}, corresponding to C–Cl stretch of acid chlorides.

The dried biomass of algal cells of *S. elongatus* after treatment with 0.001 M $AgNO_3$ was used for XRD analysis to know about the presence of silver nanoparticles and their lattice structure, i.e., whether amorphous or crystalline. The two theta positions at 46.07°, 38.06°, 32.09° and 27.70° (planes) confirm the presence of silver nanocrystals. A sharp peak at 38.06° Bragg's angle depicts the dominance of 111 planes of silver nanoparticles with a face-centred cubic structure (Fig. 6).

Antibacterial and synergistic activity of the biogenic silver nanoparticles with antibiotics

The biologically synthesized silver nanoparticles showed an inhibition zone against all the studied bacterial stains. Maximum zone of inhibition was found against *E. tarda* (13.5 ± 0.28 mm) followed by *A. hydrophila* (12.33 ± 0.33 mm), whereas *V. parahaemolyticus* exhibited the least susceptibility towards silver nanoparticles. Further, antibacterial efficacy of ofloxacin was found significantly ($P < 0.05$) higher against *A. hydrophila*. Similarly, ciprofloxacin showed a significantly ($P < 0.05$) higher zone of inhibition against *V. parahaemolyticus* and *E. tarda*. Biogenic silver nanoparticles when applied in combination with antibiotics showed a remarkable increase in the zone of inhibition (Table 1). The synergistic effects of AgNPs to antibiotics varied in a strain-specific manner (Fig. 7). The increase in size of the inhibition zone ranged between 6.84 and 23.15%. The highest (23.15%) and lowest (6.84%) increases in the diameter of the zone of inhibition were found against *E. tarda* when gentamicin (100 μg per disc) and ofloxacin were combined with silver nanoparticles.

Effect of biogenic silver nanoparticles on *Microcystis aeruginosa* and *Phormidium fragile*

The cell-free suspension of biogenic silver nanoparticle (BNP) produced after bioreduction of ionic silver by *S. elongatus* showed a pronounced effect on the reduction of the number of colonies of *M. aeruginosa* in treated water samples. There was a concentration-dependent decrease in the number of colonies in the range 1–5% BNP solution. The colonies were completely eliminated at 5% BNP concentration. The algal suspension treated with 4 and 5% BNP not only showed the disintegration of the *M. aeruginosa* colonies but also facilitated the emergence of other diverse algal species (Supplementary Figs. S1, S2). A similar trend was observed in *P. fragile* where BNP showed a strong inhibitory effect on growth and chlorophyll-a content of *P. fragile* (Table 2) with a 72.94% decrease in growth rate after exposure of the algal cells to 3% BNP solution. The concentrations 4 and 5% BNP completely inhibited growth of *P. fragile*. Chlorophyll-*a* content of *P. fragile* decreased considerably after exposure to 1–5% BNP (Table 2). Chl-*a* concentration was reduced by 84.5% at 3% BNP concentration. Further, in 4 and 5% of BNP, chlorophyll *a* could not be detected in the algal suspension.

Table 1 Inhibitory effect measured as zone of inhibition (mm) on growth of Gram-negative bacterial fish pathogens after exposure to a combination of biogenic nanosilver particle and selected antibiotics (doses: AgNPs 10^{-3} M; gentamicin and ampicillin 10 μg per disc; ofloxacin and ciprofloxacin 5 μg per disc)

Bacteria	AgNPs	Gentamicin	AgNPs + gentamicin	Ofloxacin	AgNPs + ofloxacin	Ciprofloxacin	AgNPs + ciprofloxacin	Ampicillin	AgNPs + ampicillin
A. hydrophila	12.33 ± 0.33	20.16 ± 0.16	23.3* ± 0.15	34.00 ± 0.57	37.83* ± 0.16	27.26 ± 0.13	29.20* ± 0.11	0	12.33 ± 0.17
V. parahaemolyticus	8.33 ± 0.33	21.33 ± 0.33	24.26* ± 0.17	24.16 ± 0.16	26.20 ± 0.10	25.36 ± 0.18	29.33* ± 0.16	23.3 ± 0.17	27.20* ± 0.10
E. tarda	13.5 ± 0.28	18.4 ± 0.20	22.66* ± 0.33	28.20 ± 0.20	30.13 ± 0.06	33.33 ± 0.33	36.26* ± 0.13	24.26 ± 0.17	29.30* ± 0.17

Data are presented in mean ± SE, where $n = 3$ and * depicted in rows shows significant ($P < 0.05$) difference from the used antibiotics

Discussion

Light microscopy of the population of *S. elongatus* exposed to higher concentrations, i.e., 10^{-2} and 10^{-1} M $AgNO_3$, showed the lysis of cells within 6 h of exposure time. However, in *S. elongatus* exposed to lower concentrations (10^{-3} and 10^{-4} M $AgNO_3$), the cells were not only morphologically intact but also remained viable at above concentrations. This was evident from the increase in the density of cells with time. In order to obtain higher concentration of silver nanoparticles, 10^{-3} M concentration of silver nitrate was selected for further investigations. The individual cell showed a thin layer of brown colour on the external wall surface; however, the internal cellular contents in the control (untreated) cells were devoid of the brown coloration. This observation indicates that the bioreduction of silver ions is mostly on the wall surface of the cells. There is a possibility of the intracellular reduction through various enzymatic pathways, e.g., nitrate reductase (Danhoumane et al. 2012), but the reduced silver ions do not accumulate within cells and may diffuse to the exterior of the cells where they are deposited on the outer surface of the cell wall along with the silver nanoparticles biosynthesized through the wall constituents. The observations on the populations grown in the temperature range 18–24 °C revealed that the shift in surface plasmon resonance occurred at a specific temperature, i.e., 20 °C, and a shift of even 1 °C resulted in the inhibition of bioreduction of silver ions. The findings suggest that a specific temperature requirement is a major prerequisite for the bioreduction process through *S. elongatus*.

Silver nanoparticles produced after the exposure of *S. elongatus* populations to 10^{-3} M silver nitrate solution were polydispersed with a size range of 71–201 nm. The polydispersity of nanoparticles can be attributed to the extent of bioreduction depending upon the biomolecule involved in the reduction process. Another possible explanation for the varied size of silver nanoparticles is the lower zeta potential (−9.11 mV) which may be due to the aggregation of smaller nanoparticles into larger units of multiple nanoparticles. It was noticed that the size of the particles measured by TEM was smaller than those measured by a Malvern Mastersizer. Therefore, the dimensions measured by TEM represent the actual size of the biosynthesized nanoparticles, whereas the value obtained through the Malvern Mastersizer depicts the dimensions of the aggregates of silver nanoparticles formed due to lower zeta potential. The difference in particle size of silver nanoparticles by TEM (7–12 nm) and Malvern Mastersizer 2000 (100–200 nm) may be due to the aggregation of nanoparticles during the measurement by the Mastersizer. Sonication process before measurement by TEM may lead to fragmentation of the aggregated nanoparticles in to individual small-sized particles.

In the present study, the FTIR measurements confirmed the presence of characteristic bands of various functional groups

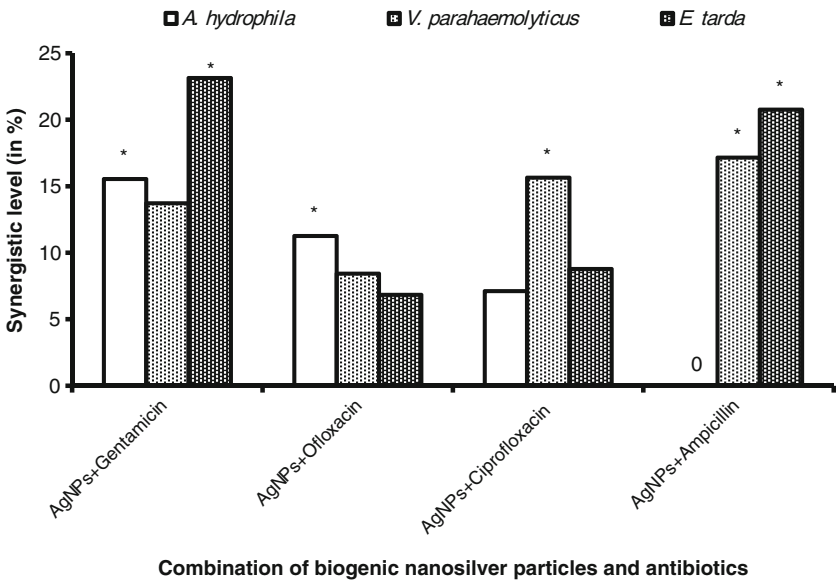

Fig. 7 Strain-specific variation in synergistic effects (%) of AgNPs and antibiotics against selected fish pathogenic bacteria

and the shifting of bands post treatment of silver nitrate confirms the involvement of these functional groups in the bioreduction process. The bands at 1325 and 1512 cm^{-1} in the spectrum of silver nanoparticle can be attributed to –C–O stretching mode and C=C chain, respectively (Schulz and Baranska 2007; Philip and Unni 2011). The characteristic peak at 1725 cm^{-1} for the treatment of silver nitrate with *Chaetomorpha linum* extract showed the presence of free amino groups contributing to the stabilization of silver nanoparticles formed after bioreduction (Philip 2010; Kannan et al. 2013). The vibrational bands corresponding to the bonds such as –C=C (ring), –C–O, –C–O–C and C=C (chain) were derived from water-soluble compounds present in *S. elongatus* extract. Hence, it may be inferred that these water-soluble biomolecules are responsible for capping and efficient stabilization.

Silver nanoparticle produced from *S. elongatus* exhibited an appreciable antibacterial activity against the fish pathogenic bacteria studied. The antibacterial activity of silver nanoparticles against several pathogenic strains with resistance against antibiotics has been documented (Rai et al. 2012). We also found resistance against ampicillin in *A. hydrophila* (Gram-negative bacterium); however, it was interesting to note that these ampicillin-resistant bacteria were sensitive to silver nanoparticles which showed an appreciable inhibitory

Table 2 Number of colonies, inhibition of growth and doubling time of *Microcystis aeruginosa* and chlorophyll-*a* content (μg mg^{-1} dry wt) of marine biofouling cyanobacterium *Phormidium fragile* after treatment with silver nitrate and diluted biogenic silver nanoparticle (BNP) solution post 10 days and 48-h exposure, respectively

Treatments[a]/algae	*Microcystis aeruginosa*			*Phormidium fragile*
Parameters	Number of colonies mL^{-1}	Specific growth rate (*k*) (day^{-1})	Generation time (days)	Chl-*a* (μg mg^{-1})
Control	1875	0.340 ± 0.012	02.02 ± 0.012	64.5 ± 3.8
Algae + silver nitrate (10^{-3} M)	0	0	–	NGD
Algae + 1% NP solution	1000	0.229 ± 0.021	3.15 ± 0.027	52.8 ± 4.2
Algae + 2% NP solution	700	0.158 ± 0.034	4.22 ± 0.021	41.4 ± 3.2
Algae + 3% NP solution	375	0.092 ± 0.008	7.53 ± 0.23	9.92 ± 0.31
Algae + 4% NP solution	125	NGD	–	NGD
Algae + 5% NP solution	0	NGD	–	NGD

NGD no growth detected

[a] 1, 2, 3, 4 and 5% NP solutions were prepared by mixing cell-free suspension 1 mL biogenic silver NP solution + 99 mL lake water with natural algal flora containing about 350 ± 20 colonies of *M. aeruginosa* per mL

effect against the above bacterial strain. The observations suggest that after a thorough screening of various pathogenic strains for their sensitivity/resistance towards specific antibiotics and metal nanoparticles, there is scope for the use of nanoparticles alone where a bacterial strain has developed resistance to multiple antibiotics. The mechanism of growth inhibitory effects of silver nanoparticles on microorganisms is not clearly understood. One possibility is that the growth inhibition may be related to the formation of free radicals from the surface of silver. Uncontrolled generation of free radicals can attack membrane lipids and lead to a breakdown of membrane function. The varying degree of efficacy of nanoparticles can be attributed to the structural difference in cell wall composition of Gram-positive and Gram-negative bacteria (Rai et al. 2012). Gram-negative bacteria have a layer of lipopolysaccharides at the exterior, followed underneath by a thin layer of peptidoglycan. Although the lipopolysaccharides are composed of covalently linked lipids and polysaccharides, there is a lack of strength and rigidity. The negative charges on lipopolysaccharides are attracted towards the weak positive charge on silver nanoparticles and can attack the Gram-negative bacteria by metal depletion (Amro et al. 2000; Ahmad et al. 2003). Shahverdi et al. (2007) investigated the combined effects of silver nanoparticles with antibiotics like penicillin G, amoxicillin, erythromycin, clindamycin and vancomycin for both Gram-negative and Gram-positive human pathogenic bacteria. They noticed an increased efficacy of antibiotics in the presence of silver nanoparticle against *Escherichia coli* and *Staphylococcus aureus*. The ampicillin molecules act on the cell wall, which leads to cell wall lysis and thus increases the penetration of AgNPs into the bacterium. The AgNP–ampicillin complex reacts with DNA and prevents DNA unwinding, which results in more serious damage to bacterial cells (Batarseh 2004). Our results endorse the synergistic effect of biogenic nanoparticles (produced from *S. elongatus* by live cells in culture medium) with different antibiotics against pathogenic Gram-negative bacteria of fish which ultimately enhances the efficacy of the antibiotic against pathogenic strains. The possible mechanism of higher efficacy or increased activity of antibiotics may be due to higher attachment of antibiotic molecules to the surface of AgNPs. Since gentamicin is an aminoglycoside, the hydroxyl group tends to bind with positively charged AgNPs and amino groups stabilize it. Similarly, ampicillin having more ketone and hydroxyl groups may facilitate binding of a larger number of antibiotic molecules with AgNPs, resulting in higher antimicrobial activity (Fayaz et al. 2010). Among the strains, the highest enhancement in efficacy was observed for gentamicin against *E. tarda*. *Aeromonas hydrophila* was found resistant to ampicillin but it showed a considerable inhibitory effect on ampicillin-resistant strains, suggesting that nanoparticles alone can inhibit the growth of the above bacteria. This phenomenon was reported earlier also where the antibacterial activities of ampicillin, kanamycin, erythromycin and chloramphenicol increased in the presence of silver nanoparticles against test strains (Shahverdi et al. 2007; Fayaz et al. 2010).

The inhibition of growth of the marine cyanobacterium *P. fragile* and the freshwater cyanobacterium *M. aeruginosa* can be attributed to the loss of membrane integrity (Jung et al. 2008). AgNP-treated samples of *M. aeruginosa* showed that the inhibition of growth of the cyanobacterium was due to loss of the integrity of the colonies which was evident from the disruption of the gelatinous matrix which envelops the cells of the colony. Once the colony is disintegrated, the embedded cells are released into the medium but do not form new colonies and are disintegrated within 48 h. The reappearance of algal diversity (*Pediastrum* sp., *Scenedesmus* sp., *Selenastrum* sp., *Nitzschia* sp., *Synedra ulna*, etc.) can be attributed to selective disintegration of *Microcystis* colonies by the biogenic silver nanoparticles. The findings of the present investigation endorse an earlier report by Chaturvedi and Verma (2015) on algicidal effects of biogenic silver nanoparticles on cyanobacteria.

The toxicity of nanoparticles is considered to be a major issue in their wider application. Although there are limited reports on the toxicity of nanoparticles, an earlier report on toxicity of nanoparticles on fish indicates that silver nanoparticles were approximately four times less toxic than silver ion, indicating that nanosized forms of silver are less toxic than its soluble form (Massarsky et al. 2013). Overall, it is concluded the silver nanoparticles synthesized through green pathway using cyanobacteria are effective against waterborne fish pathogens and bloom-forming and biofouling cyanobacteria and their efficacy is equal to silver nanoparticles synthesized via synthetic chemical-based pathways. Further, like for human pathogens, biosynthesized silver nanoparticles are effective against fish pathogens and show an appreciable synergy with selected antibiotics against fish pathogenic bacteria. Furthermore, the efficacy of silver nanoparticles against an ampicillin-resistant strain of *A. hydrophila* highlights the standalone potentiality of biogenic silver nanoparticle as a tool for controlling the growth of drug-resistant bacteria.

Acknowledgements The authors are thankful to the Director of ICAR-Central Institute of Fisheries Education and Indian Council of Agricultural Research for the support. The first author is thankful to the members of her advisory committee for valuable inputs.

References

Ahmad A, Mukherjee P, Senapati P, Mandal D, Islam Khan M, Kumar R (2003) Extracellular biosynthesis of silver nanoparticles using the fungus *Fusarium oxysporum*. Colloid Surf B 28:313–318

Amro NA, Kotra LP, Wadu-Mesthrige K, Bulychev A, Mobashery S, Liu G (2000) High resolution atomic force microscopy studies of the *Escherichia coli* outer membrane: structural basis for permeability. Langmuir 16:2789–2796

Batarseh KI (2004) Anomaly and correlation of killing in the therapeutic properties of silver (I) chelation with glutamic and tartaric acids. J Antimicrob Chemother 54:546–548

Bauer RW, Kirby MDK, Sherris JC, Turck M (1966) Antibiotic susceptibility testing by standard single disc diffusion method. Am J Clin Pathol 45:493–496

Chaturvedi V, Verma P (2015) Fabrication of silver nanoparticles from leaf extract of *Butea monosperma* (flame of forest) and their inhibitory effect on bloom-forming cyanobacteria. Biores Bioproc 2(1):18

Cho KH, Park JE, Osaka T, Park SG (2005) The study of antimicrobial activity and preservative effects of nanosilver ingredient. Electrochim Acta 51:956–960

Con TH, Loan DK (2011) Preparation of silver nano-particles and use as a material for water sterilization. Environ Asia 4:62–66

Danhoumane AS, Djediat C, Yepremian C, Coute A, Fievet F, Coradin T, Brayner R (2012) Species selection for the design of gold nanobioreactor by photosynthetic organisms. J Nanopart Res 14:883

Dash A, Singh AP, Chaudhary BR, Singh SK, Dash D (2012) Effect of silver nanoparticles on growth of eukaryotic green algae. Nano-Micro Let 4:158–165

Fayaz AM, Balaji K, Girilal M, Yadav J, Kalaichelvan PT, Venketsan R (2010) Biogenic synthesis of silver nanoparticles and their synergistic effect with antibiotics: a study on Gram-positive and Gram-negative bacteria. Nanomedicine 6:103–109

Govindaraju K, Basha SK, Kumar VG, Singaravelu G (2008) Silver, gold and bimetallic nanoparticles production using single cell protein (*Spirulina platensis*) Geitler. J Material Sci 43:5115–5122

Guillard RRL (1973) Methods for microflagellates and nannoplankton. In: Stein JR (ed) Handbook of phycological methods: culture methods and growth measurements. Cambridge University Press, Cambridge, pp 69–85

Guillard RRL, Ryther JH (1962) Studies of marine planktonic diatoms. I. *Cyclotella nana* Hustedt and *Detonula confervacea* Cleve. Can J Microbiol 8:229–239

Heuer OE, Kruse H, Grave K, Karunasagar I, Angulo J (2009) Human health consequences of use of antimicrobial agents in aquaculture. Clin Infect Dis 49:1248–1253

Jung WK, Koo HC, Kim KW, Shin S, Kim SH, Park YH (2008) Antibacterial activity and mechanism of action of the silver ion in *Staphylococcus aureus* and *Escherichia coli*. Appl Environ Microbiol 74:2171–2178

Kannan RR, Arumugam R, Ramya D, Manivannan K, Anantharaman P (2013) Green synthesis of silver nanoparticles using marine macroalga *Chaetomorpha linum*. Appl Nanosci 3:229–233

Khlebtsov NG, Dykman LA (2010) Optical properties and biomedical applications of plasmonic nanoparticles. J Quant Spectrosc Radiat Transf 111:–35

Koonse B, Burkhardt W, Chirtel S, Hoskin GP (2005) *Salmonella* and the sanitary quality of aquacultured shrimp. J Food Prot 68:2527–2532

Kratz WA, Myers J (1955) Nutrition and growth of several blue-green algae. Amer J Bot:282–287

Martinez-Gutierrez F, Boegli L, Agostinho A, Sánchez EM, Bach H, Ruiz F, James G (2013) Anti-biofilm activity of silver nanoparticles against different microorganisms. Biofouling 29:651–660

Massarsky A, Dupuis L, Taylor J, Eisa-Beygi S, Strek L, Trudeau VL, Moon TW (2013) Assessment of nanosilver toxicity during zebrafish (*Danio rerio*) development. Chemosphere 92:59–66

Moran R (1982) Formulae for determination of chlorophyllous pigments extracted with *N*, *N*-dimethylformamide. Plant Physiol 69:1376–1381

Muruganandam S, Anbalagan G, Murugadoss G (2014) Optical, electrochemical and thermal properties of Co^{2+}-doped CdS nanoparticles using polyvinylpyrrolidone. Appl Nanosci. doi:10.1007/s13204-014-0313-6

Park MH, Kim KH, Lee HH, Kim JS, Hwang SJ (2010) Selective inhibitory potential of silver nanoparticles on the harmful cyanobacterium *Microcystis aeruginosa*. Biotechnol Lett 32:423–428

Paul K, Bag BG, Samanta K (2014) Green coconut (*Cocos nucifera* Linn.) shell extract mediated size controlled green synthesis of polyshaped gold nanoparticles and its application in catalysis. Appl Nanosci 4:769–775

Philip D (2010) Green synthesis of gold and silver nanoparticles using *Hibiscus rosa sinensis*. Phys E 42:1417–1424

Philip D, Unni C (2011) Extracellular biosynthesis of gold and silver nanoparticles using Krishna tulsi (*Ocimum sanctum*) leaf. Phys E 43:1318–1322

Prasad TNVKV, Kambala VSR, Naidu R (2013) Phyconanotechnology: synthesis of silver nanoparticles using brown marine algae *Cystophora moniliformis* and their characterization. J Appl Phycol 25:177–182

Rai MK, Deshmukh SD, Ingle AP, Gade AK (2012) Silver nanoparticles: the powerful nano-weapon against multidrug-resistant bacteria. J Appl Microbiol 112:841–852

Ravichandran R (2009) Nanoparticles in drug delivery: potential green nanobiomedicine applications. Int J Nanotechnol Biomed 1:108–130

Roychoudhury P, Gopal PK, Paul S, Pal R (2016) Cyanobacteria assisted biosynthesis of silver nanoparticles—a potential antileukemic agent. J Appl Phycol 28:3387–3394

Satapathy S, Shukla SP, Sandeep KP, Singh AR, Sharma N (2015) Evaluation of the performance of an algal bioreactor for silver nanoparticle production. J Appl Phycol 27:285–291

Schulz H, Baranska M (2007) Identification and quantification of valuable plant substances by IR and Raman spectroscopy. Vib Spectrosc 43:13–25

Schwartz T, Kohnen W, Jansen B, Obst U (2003) Detection of antibiotic-resistant bacteria and their resistance genes in wastewater, surface water, and drinking water biofilms. FEMS Microbiol Ecol 43:325–335

Shahverdi AR, Fakhimi A, Shahverdi HR, Minaian S (2007) Synthesis and effect of silver nanoparticles on the antibacterial activity of different antibiotics against *Staphylococcus aureus* and *Escherichia coli*. Nanomedicine 3:168–171

Sharma VK, Yngard RA, Lin Y (2009) Silver nanoparticles: green synthesis and their antimicrobial activities. Adv Colloid Interf Sci 145: 83–96

Sharma A, Sharma S, Sharma K, Chetri SP, Vashishtha A, Singh P, Kumar R, Rathi B, Agrawal V (2016) Algae as crucial organisms in advancing nanotechnology: a systematic review. J Appl Phycol 28:1759–1774

Singaravelu G, Arockiamary JS, Kumar VG, Govindaraju K (2007) A novel extracellular synthesis of monodisperse gold nanoparticles using marine alga, *Sargassum wightii* Greville. Colloids Surfaces B 57:97–101

Stanier RY, Kunisawa R, Mandel M, Cohen-Bazire G (1971) Purification and properties of unicellular blue-green algae (order Chroococcales). Bact Rev 35:171–205

Van Boeckel TP, Brower C, Gilbert M, Grenfell BT, Levin SA, Robinson TP, Teillant A, Laxminarayan R (2015) Global trends in antimicrobial use in food animals. Proc Nat Acad Sci 112:5649–5654

Venkatesan P, Santhanalakshmi J (2014) Synthesis, characterisation and catalytic activity of gold and silver nanoparticles in the biosensor application. J Exp Nanosci 9:293–298

Vieira AP, Stein EM, Andreguetti DX, Colepicolo P, da Costa Ferreira AM (2016) Preparation of silver nanoparticles using aqueous extracts of the red algae *Laurencia aldingensis* and *Laurenciella* sp. and their cytotoxic activities. J Appl Phycol 28:2615–2622

World Health Organization (WHO) (2005) Critically important antibacterial agents for human medicine; for risk management strategies of non human use. Report of a WHO working group consultation, Canberra, Australia, 15–18 February

Zhang M, Zhang K, De Gusseme B, Verstraete W, Field R (2014) The antibacterial and anti-biofouling performance of biogenic silver nanoparticles by *Lactobacillus fermentum*. Biofouling 30:347–357